A Protein-Counting Mechanism for Telomere Length Regulation in Yeast

Stéphane Marcand, *et al.*

Science **275**, 986 (1997);
DOI: 10.1126/science.275.5302.986

teins only within the BH3 region. In contrast, other Bcl-2–related proteins such as Bak or Bax are predicted to have more extensive structural similarities to Bcl-x_L. For these proteins, our studies suggest that a structural change may be required for the BH3 region to participate in dimerization.

REFERENCES AND NOTES

1. C. B. Thompson, *Science* **267**, 1456 (1995).
2. J. C. Reed, *J. Cell Biol.* **124**, 1 (1994).
3. X.-M. Yin, Z. N. Oltvai, S. J. Korsmeyer, *Nature* **369**, 321 (1994).
4. Z. N. Oltvai and S. J. Korsmeyer, *Cell* **79**, 189 (1994).
5. M. Hanada, C. Aimé-Sempé, T. Sato, J. C. Reed, *J. Biol. Chem.* **270**, 11962 (1995).
6. E. H.-Y. Cheng, B. Levine, L. H. Boise, C. B. Thompson, J. M. Hardwick, *Nature* **379**, 554 (1996).
7. T. Chittenden *et al.*, *EMBO J.* **14**, 5589 (1995).
8. J. M. Boyd *et al.*, *Oncogene* **11**, 1921 (1995).
9. H. Zha, C. Aimé-Sempé, T. Sato, J. C. Reed, *J. Biol. Chem.* **271**, 7440 (1996).
10. J. Hunter and T. G. Parslow, *ibid.*, p. 8521.
11. S. W. Muchmore *et al.*, *Nature* **381**, 335 (1996).
12. T. Sato *et al.*, *Proc. Natl. Acad. Sci. U.S.A.* **91**, 9238 (1994).
13. T. W. Sedlak, *ibid.* **92**, 7834 (1995).
14. The binding affinities of peptides to full-length Bcl-x_L were measured from the fluorescence emission of the Trp residues of Bcl-x_L as a function of increasing peptide concentration. The excitation and emission wavelengths were 290 and 340 nm, respectively.
15. Unlabeled peptide (GQVGRQLAIIGDDINR) and a peptide uniformly ^{15}N-,^{13}C-enriched for the Gly, Ala, Val, Leu, and Ile residues were purchased from PeptidoGenic Research (Livermore, CA) and purified by reversed-phase high-performance liquid chromatography on a C8 column. NMR samples (1 to 3 mM) of a 1:1 protein-peptide complex were prepared in a 10 mM sodium phosphate buffer (pH 6.5) in ^2H_2O or a 9:1 mixture of H_2O and ^2H_2O.
16. The deletion mutant of Bcl-x_L used in the NMR studies lacks the putative COOH-terminal transmembrane region and residues 45 to 84, which constitute a flexible loop previously shown to be dispensible for the antiapoptotic activity of Bcl-x_L (*11*). The deletion mutant of Bcl-x_L was constructed from the expression vector for Bcl-x_L (residues 1 to 209) (*11*) by a procedure similar to that of M. P. Weiner *et al*. [*Gene* **151**, 119 (1994)]. Residue numbers correspond to full-length Bcl-x_L. Thus, in the Δ(45–84)Bcl-x_L construct used in this study, residues 44 and 85 are sequential. The Δ(45–84)Bcl-x_L construct also has four additional NH_2-terminal residues (numbers −3 to 0) due to cloning artifacts. We prepared uniformly ^{15}N- and ^{15}N-,^{13}C-labeled proteins by growing the *Escherichia coli* strain HMS174(DE3) overexpressing Bcl-x_L on a minimal medium containing $^{15}NH_4Cl$ with or without [U-^{13}C]glucose. We prepared uniformly ^{15}N-,^{13}C-labeled and fractionally deuterated protein by growing the cells in 75% ^2H_2O. The recombinant protein was purified by affinity chromatography on a nickel-IDA column (Invitrogen) followed by ion-exchange chromatography on an S-Sepharose column.
17. NMR spectra were acquired at 30°C on a Bruker DMX500 or AMX600 NMR spectrometer. The ^{1}H, ^{13}C, and ^{15}N resonances of the backbone and side chains were obtained with a sample containing the (U-^{15}N-,^{13}C)-labeled and 75% deuterated protein as described [T. Yamazaki, W. Lee, S. H. Arrowsmith, D. R. Muhandiram, L. E. Kay, *J. Am. Chem. Soc.* **116**, 11655 (1994); G. M. Clore and A. M. Gronenborn, *Methods Enzymol.* **239**, 349 (1994)]. The methyl groups of Val and Leu residues were stereospecifically assigned [D. Neri, T. Szyperski, G. Otting, H. Senn, K. Wüthrich, *Biochemistry* **28,** 7510 (1989)]. Distance restraints were obtained from ^{15}N- or ^{13}C-resolved 3D NOE spectra, and ϕ dihedral angle restraints were measured from $^3J_{H^N,H^\alpha}$ coupling constants [H. Kuboniwa, S. Grzesiek, F. Delaglio, A. Bax *J. Biomol. NMR* **4,** 871 (1994)]. To assign the NMR resonances of the peptide and obtain intra- and intermolecular distance restraints, we acquired 2D and 3D ^{15}N-,^{13}C-filtered experiments on a sample with (U-^{15}N-,^{13}C)-labeled protein and unlabeled peptide. Additional distance restraints from ^{15}N- and ^{13}C-separated NOE experiments were obtained with a sample of unlabeled protein complexed to the Bak peptide uniformly ^{15}N- and ^{13}C- labeled for Gly, Ala, Val, Leu, and Ile. The structure calculations were based on a distance geometry and simulated annealing protocol [J. Kuszewski, M. Nilges, A. T. Brünger *J. Biomol. NMR* **2,** 33 (1992)] with the program X-PLOR [A. T. Brünger, *X-PLOR Version 3.1*, Yale University, New Haven, CT (1992)]. NOE-derived distance restraints with a square-well potential (F_{noe} = 50 kcal mol^{-1} Å^{-2}) were used after each was categorized as strong (1.8 to 3.0 Å), medium (1.8 to 4.0 Å), or weak (1.8 to 5.0 Å) on the basis of the NOE intensity. An additional 138 distance restraints were included for 69 hydrogen bonds identified from the slowly exchanging amides and given bounds of 1.8 to 2.3 Å (H-O) and 2.8 to 3.3 Å (N-O). No distance restraint was violated by more than 0.35 Å in any of the final structures. For the ensemble, the residual NOE rmsd was 0.009 ± 0.003 Å and the E_{noe} was 15 ± 3 kcal mol^{-1}. Torsional restraints were applied to 71 ϕ angles (including five for the peptide) with values of −60 ± 40° (F_{cdih} = 200 kcal mol^{-1} rad^{-2}) for $^3J(H^N,H^\alpha)$ for coupling constants <5.8 Hz in α-helical regions. No torsional angle restraint was violated by more than 5° in any of the final structures. For the ensemble, the residual torsional rmsd was 0.11 ± 0.06° and the E_{cdih} was 0.1 ± 0.0 kcal mol^{-1}. The covalent geometries were well satisified as indicated by a small total energy (137 ± 10 kcal mol^{-1}). Although the Lennard-Jones potential was not used during any refinement stage, the final structures exhibited good van der Waals geometries as illustrated by an $E_{L\text{-}J}$ of −1104 ± 12 kcal mol^{-1}.
18. The rmsd between the NMR structures of free and complexed Bcl-x_L for the C$^\alpha$ atoms within the common regular elements of secondary structure is 1.7 Å. When complexed to the Bak peptide, residues 101 to 103 form an extension of the second α helix, the third helix in Bcl-x_L is reduced to a single helical turn, and residues 198 to 205 form an additional helix.
19. M. Eberstadt, M. Sattler, S. W. Fesik, unpublished data.
20. B. Chang, A. J. Minn, C. B. Thompson, unpublished data.
21. M. J. Carson, *J. Mol. Graph.* **5**, 103 (1987).

22. Supported in part by research grants POI AI35294 (C.B.T.) and R37 CA48023 (C.B.T.) from the National Institutes of Health. Coordinates for the averaged minimized NMR structure of the Bcl-x_L–Bak peptide complex have been deposited in the Brookhaven Protein Data Bank (accession number 1BXL).

15 July 1996; accepted 9 December 1996

A Protein-Counting Mechanism for Telomere Length Regulation in Yeast

Stéphane Marcand,* Eric Gilson, David Shore†

In the yeast *Saccharomyces cerevisiae*, telomere elongation is negatively regulated by the telomere repeat–binding protein Rap1p, such that a narrow length distribution of telomere repeat tracts is observed. This length regulation was shown to function independently of the orientation of the telomere repeats. The number of repeats at an individual telomere was reduced when hybrid proteins containing the Rap1p carboxyl terminus were targeted there by a heterologous DNA-binding domain. The extent of this telomere tract shortening was proportional to the number of targeted molecules, consistent with a feedback mechanism of telomere length regulation that can discriminate the precise number of Rap1p molecules bound to the chromosome end.

Telomeres, the ends of linear eukaryotic chromosomes, are essential structures formed by specific protein-DNA complexes that protect chromosomal termini from degradation and fusion (*1*). One of the essential functions of telomeres is to allow the complete replication of chromosome ends, which cannot be accomplished by known DNA polymerases (*2*). The progressive loss of DNA that would occur after each round of replication is balanced by a ribonucleoprotein terminal transferase enzyme called telomerase, which specifically extends the 3′ G-rich telomeric strand in an RNA-templated reaction (*3*). In most organisms, telomeric DNA consists of a tandem array of short repeats. In yeast, the telomeric DNA is organized in a nonnucleosomal structure based on an array of the telomere repeat–binding protein Rap1p (*4, 5*).

In the human germline, cells express telomerase and maintain a constant average telomere length. This initial size appears to determine the replicative life-span of somatic cells, in which telomerase activity is usually undetectable and telomere repeats are progressively lost at each cell division (*6*). In unicellular organisms like *S. cerevisiae*, telomere length is kept within a narrow size distribution, specific for a given strain,

S. Marcand, Department of Microbiology, College of Physicians and Surgeons, Columbia University, New York, NY 10032, USA, and Laboratoire de Biologie Moléculaire et Cellulaire, Ecole Normale Supérieure de Lyon, 69364 Lyon Cédex 07, France.
E. Gilson, Laboratoire de Biologie Moléculaire et Cellulaire, Ecole Normale Supérieure de Lyon, UMR49 CNRS/ENSL, 69364 Lyon Cédex 07, France.
D. Shore, Department of Microbiology, College of Physicians and Surgeons, Columbia University, New York, NY 10032, USA, and Department of Molecular Biology, University of Geneva, CH-1211 Geneva 4, Switzerland.

*Present address: Ecole Normale Supérieure de Lyon, 69364 Lyon Cédex 07, France.
†To whom correspondence should be addressed (at University of Geneva). E-mail: David.Shore@molbio.unige.ch

and does not appear to vary with growth conditions or culturing time (*7*). Telomere length regulation can be viewed as the result of a balance between elongation and shortening. It has been proposed that this equilibrium is determined by negative regulation of telomerase activity by the telomere itself when a specific threshold length is reached (*8, 9*), or by a progressive increase in the frequency of intrachromatid terminal excision as a function of repeat length (*10*). Moreover, the narrow distribution of telomere lengths observed in vivo supports the existence of a length-sensing mechanism capable of efficiently discriminating even small differences in tract length.

To investigate the molecular nature of this telomere length-sensing mechanism, we used a telomere "healing" assay in which a *URA3* marker gene and an adjacent short stretch of TG_{1-3} sequence [~80 base pairs (bp)] were transformed into yeast cells and, by homologous recombination, replaced the left extremity of chromosome VII beyond the *ADH4* gene (*11*) (Fig. 1A). During this process, the short TG_{1-3} tract is extended by telomerase (*3*) to yield a telomere tract whose length is characteristic of the host strain. This assay allowed us to insert sequences of interest adjacent to a single telomere and to determine their effect on the length of that telomere with a *URA3* probe.

We first inserted an additional 80-bp fragment of native telomeric repeats adjacent to the *URA3* marker and in the same orientation as the repeats on the starting plasmid (*12*) (Fig. 1A). As shown in Fig. 1B, this insert only slightly increased the size of the Hind III telomeric restriction fragment, indicating that the distal TG_{1-3} tract was ~70 to 80 bp shorter than in the absence of the insert (220 to 230 bp versus 300 bp). Therefore, despite being separated from the telomere by a linker sequence of 40 bp, the 80-bp TG_{1-3} insert appears to be recognized as part of the telomere repeat tract, whose total length is then regulated to the original value (300 bp).

When the 80-bp telomeric repeats were inserted in the opposite orientation relative to the native telomere, the size of the telomeric *URA3* restriction fragment was also only slightly increased (~30 bp, Fig. 1B), indicating that ~90 bp less TG_{1-3} sequence had been added in the healing process, relative to the minus-insert control, to compensate for the additional TG_{1-3} tract. To rule out the possibility that the inserted (internal) repeats had been deleted, we took advantage of the Bam HI restriction site at the junction between the two telomeric sequences (Fig. 1A). Cutting with Hind III and Bam HI released a 1240-bp fragment, which was, as expected, 120 bp longer than in the absence of an insert (Fig. 1B). This result indicates that an insert of the expected size was present at the telomere, and thus that the distal telomeric tract sequence was shorter. We repeated this experiment by inserting a 270-bp telomeric fragment adjacent to the original 80-bp tract but in the opposite orientation. In this situation, the resulting distal TG_{1-3} tract was only 120 to 130 bp long (Fig. 1B), indicating that most of the internal 270-bp repeat (~180 to 200 bp) had been counted as part of the telomere, even though it was misoriented. In an independent experiment with the two 80-bp insert constructs, we used restriction sites positioned closer to the telomere (Apa I and Eco RV) to increase the precision of the measurements. The estimated sizes of the TG_{1-3} tracts were very similar to those determined with Hind III (Fig. 1C), which confirmed the observed difference in tract length caused by the 80-bp insert. Taken together, these results suggest that the number of telomere repeats per se, regardless of their orientation, is regulated in yeast.

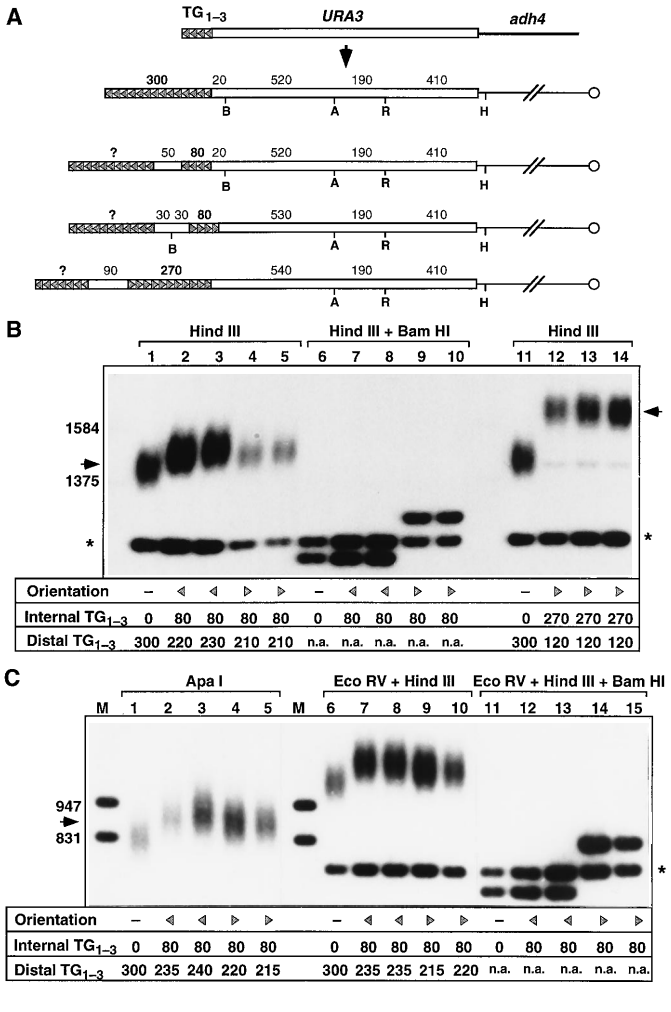

Fig. 1. Telomere length regulation is independent of telomere repeat tract orientation. (**A**) Schematic representation (top two lines) of the initial telomere healing fragment and its conversion in yeast cells into a stable telomere with an average TG_{1-3} tract length of 300 bp (strain Lev7). The bottom three lines depict the chromosomal structure for transformants with additional TG_{1-3} inserts at the Bam HI site of the starting plasmid: an 80-bp TG_{1-3} insert in telomeric orientation (strains Lev165 and Lev166), an 80-bp TG_{1-3} insert in reverse orientation (strains Lev143 and Lev144), and a 270-bp TG_{1-3} insert in reverse orientation (strains Lev153, Lev154, and Lev155). The positions of the Hind III (H), Eco RV (R), Apa I (A), and Bam HI (B) sites and the distance between the restriction sites and the TG_{1-3} repeats are indicated. The orientations of the telomeric sequences are represented by multiple arrowheads. (**B**) Genomic DNA from yeast strains Lev7 (lanes 1, 6, and 11), Lev165 (lanes 2 and 7), Lev166 (lanes 3 and 8), Lev143 (lanes 4 and 9), Lev144 (lanes 5 and 10), Lev153 (lane 12), Lev154 (lane 13), and Lev155 (lane 14) were digested with Hind III (lanes 1 to 5 and 11 to 14) or with Hind III and Bam HI (lanes 6 to 10), separated by electrophoresis on 0.9% agarose gels, and blotted onto a nitrocellulose membrane. The membrane was probed with a 1.16-kb Hind III *URA3* fragment. The median length of the telomeric restriction fragment was measured with Image-Quant, using the nontelomeric 1160-bp *ura3-1* fragment as an internal control for each lane; 1140 bp (no insert), 1270 bp (with an 80-bp TG_{1-3} insert), or 1500 bp (with a 270-bp TG_{1-3} insert) was subtracted from this value to give the indicated size of the distal TG_{1-3} tract. The arrow and the asterisk indicate the telomeric restriction fragment and the nontelomeric 1.1-kb Hind III *ura3-1* fragment, respectively; positions of size markers of 1584 and 1375 bp (not shown) are indicated. At the bottom, the relative orientation of the internal TG_{1-3} repeats and the sizes of the internal and distal TG_{1-3} repeats are indicated. (**C**) Genomic DNA from yeast strains Lev7 (lanes 1, 6, and 11), Lev165 (lanes 2, 7, and 12), Lev166 (lanes 3, 8, and 13), Lev143 (lanes 4, 9, and 14), and Lev144 (lanes 5, 10, and 15) were digested with Apa I (lanes 1 to 5), with Eco RV and Hind III (lanes 6 to 10), or with Eco RV, Hind III, and Bam HI (lanes 10 to 15). The asterisk indicates the nontelomeric 0.75-kb Eco RV–Hind III *ura3-1* fragment. M, size markers of 947 and 831 bp.

Because yeast telomeric repeats contain multiple binding sites for Rap1p (*13*), we asked whether it might be the actual number of Rap1p molecules bound at the chromosome end, rather than the repeat tract length, that is kept constant. We replaced the internal TG_{1-3} repeat inserts with binding sites for Gal4p (UAS_G, Fig. 2A), and expressed in these cells hybrids containing the COOH-terminus of Rap1p (amino acids 653 to 827) fused to the Gal4p DNA-binding domain [Gbd/Rap1(653–827), Fig. 2B] (*14*). We chose this region of Rap1p because deletion of these sequences from the native protein essentially abolishes telomere length control (9). When Gbd/Rap1(653–827) was expressed in a strain with four UAS_G sites at telomere VII-L, the median length of the telomere repeat tract was reduced from 310 to 240 bp (Fig. 2C). The Gbd control did not significantly affect telomere length, as expected. Moreover, in the absence of UAS_G sites, the Gbd/Rap1 hybrid had no effect, which demonstrated that the site of action for the hybrid protein is the targeted telomere (*15*).

To examine the specificity of Gbd/Rap1 action on telomere length, we used a *rap1-12* allele, a double missense mutation at residues 726 and 727 of the protein. This mutation causes a 100- to 150-bp increase in telomere length, indicating a partial loss of telomere length control (*16*). In a *rap1-12* background, targeting of the Rap1p wild-type COOH-terminus at a specific telomere markedly reduced its length (Fig. 2D) while leaving the rest of the telomeres in the cell unchanged (*17*). As in a wild-type background, no shortening was observed in the absence of UAS_G sites or with the Gbd control. However, when the *rap1-12* mutation was present in the hybrid protein (Gbd/rap1-12), the mutant hybrid protein had a much smaller effect on telomere length in a *RAP1* or *rap1-12* background (Fig. 2, C and D). These results strongly suggest that the targeted Gbd/Rap1 hybrids (both mutant and wild type) behave in a manner similar or identical to their respective native (full-length) counterparts with respect to telomere length control.

The ability of the COOH-terminal region of Rap1p to reduce telomere length when bound to the centromeric side of a telomere suggests that the number of Rap1p COOH-terminal domains assembled at an individual telomere is regulated. To test this idea more directly, we expressed the Gbd/Rap1(653–827) hybrid in a series of strains with increasing numbers of UAS_G sites inserted at telomere VII-L. In a wild-type cell expressing Gbd/Rap1(653–827), but not Gbd alone, a single UAS_G site reduced the median length of the targeted telomere by an average of 30 bp. A second UAS_G site reduced the length by a further 20 bp, whereas the addition of a third and fourth UAS_G site had a weaker effect, causing an additional average reduction of somewhat less than 10 bp per site; the significance of this latter effect is uncertain (Fig. 3, A and C). In a *rap1-12* mutant background, where telomeres are longer than in the wild type, the incremental shortening caused by each additional UAS_G site bound by the Gbd/Rap1 hybrid was more clearly seen (Fig. 3, B and C). In presence of Gbd/Rap1, with the first and second UAS_G sites, telomere

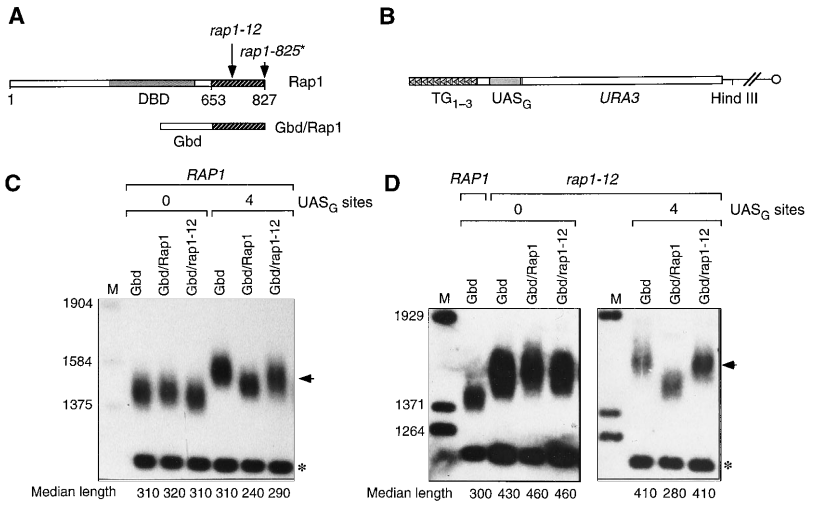

Fig. 2. Targeting several Rap1p COOH-terminal domains to the internal side of a telomere repeat tract reduces its length. (**A**) Schematic representation of the Rap1 protein and the Gbd/Rap1 hybrid protein. The positions of the *rap1-12* and *rap1-825** mutations and of the Rap1p DNA-binding domain (DBD) are indicated. (**B**) Schematic representation of telomere VII-L marked with *URA3* and UAS_G sites. The *URA3* gene is transcribed toward the telomere. (**C**) Strains Lev7 (no UAS_G sites) and Lev8 (four UAS_G sites) were cotransformed with sp17 (*RAP1*) and with pSB362 (pGbd), pSB136 (pGbd/Rap1), or pSB341 (pGbd/rap1-12). (**D**) Strains Lev7 (no UAS_G sites) and Lev8 (four UAS_G sites) were cotransformed with sp103 (*rap1-12*) and with pSB362 (pGbd), pSB136 (pGbd/Rap1), or pSB341 (pGbd/rap1-12). Genomic DNA was digested with Hind III and analyzed as described in Fig. 1. In (C) and (D), the arrow and the asterisk indicate the position of the telomeric restriction fragment and the nontelomeric 1.1-kb Hind III *ura3-1* fragment, respectively; the median length of the TG_{1-3} tract is indicated below each lane and was calculated by subtracting 1140 bp (no UAS_G sites) or 1260 bp (four UAS_G sites) from the median size of the telomeric restriction fragment.

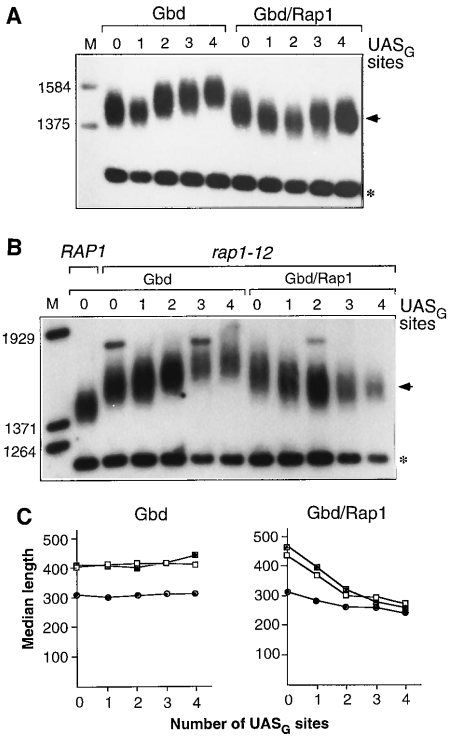

Fig. 3. The length reduction caused by Gbd/Rap1 is proportional to the number of targeted molecules. (**A**) Strains Lev7 (no UAS_G sites), Lev130 (one UAS_G site), Lev132 (two UAS_G sites), Lev134 (three UAS_G sites), and Lev8 (four UAS_G sites) were cotransformed with sp17 (*RAP1*) and either pSB362 (pGbd) or pSB136 (pGbd/Rap1). (**B**) Strains Lev7 (no UAS_G sites), Lev130 (one UAS_G site), Lev132 (two UAS_G sites), Lev134 (three UAS_G sites), and Lev8 (four UAS_G sites) were cotransformed with sp17 (*rap1-12*) and either pSB362 (pGbd) or pSB136 (pGbd/Rap1). Telomere repeat tract lengths were analyzed as above. The RAP1 lane contained Lev7 transformed only with pSB362. (**C**) The median telomere lengths in a *RAP1* background (●) were calculated by averaging four independent experiments. The SD for each mean is <15 bp. The median telomere lengths in the *rap1-12* background (■) and *rap1-825** background (□) were derived from a single experiment. With one, two, or three UAS_G sites, the median length of the TG_{1-3} tract was calculated by subtracting 1175, 1210, or 1240 bp, respectively, from the median size of the telomeric restriction fragment. In (A) and (B), the arrow and asterisk have the same meanings as in Fig. 2.

length shortened by 70 bp per site. With the addition of a third and fourth UAS_G site, the shortening was again relatively smaller but significant, approximately 30 bp per site (*18*). Similarly, in cells bearing the *rap1-825** allele [a four–amino acid insertion at position 825 (*19*)], Gbd/Rap1 reduced the median length of the targeted telomere in proportion to the number of UAS_G sites (Fig. 3C; see below).

In the yeast *S. cerevisiae*, genes inserted adjacent to a telomere can be transcriptionally silenced (*11*). This telomeric position effect (TPE) requires the same COOH-terminal region of Rap1p involved in telomere length regulation, as well as two proteins (Sir3p and Sir4p) that interact with this domain (*19*, *20*). Moreover, targeting of the COOH-terminal domain Gbd/Rap1 hybrid establishes silencing (*21*). To clarify the link between telomeric silencing and telomere length regulation, we first asked whether silencing is necessary for telomere length regulation by Gbd/Rap1. In *sir4* mutant cells, silencing is abolished and telomeres are slightly shorter (*22*). However, targeting of Rap1p COOH-terminal domains in a *sir4* mutant further reduced telomere length without restoring silencing (*17*), and thus telomere length regulation by Rap1p does not require silencing.

We also asked whether, in a *rap1* mutant strain partially defective for TPE and telomere length regulation, the reestablishment of TPE by targeting of Gbd-Sir hybrids (*23*, *24*) is sufficient to restore normal telomere length regulation. Silencing of the *URA3* gene present at telomere VII-L was quantified by the ability of cells to grow on medium containing 5-fluoroorotic acid (5-FOA), which kills cells expressing the *URA3* gene. Cells bearing the *rap1-825** allele display a partial defect in telomere length regulation (median telomere length rises from 300 to 410 bp) and silencing [the average proportion of FOA-resistant (FOA^R) cells drops from 59 to 0.6%]. As expected, Gbd/Rap1, in the presence of four UAS_G sites, reduced the median length of the targeted telomere to 290 bp and simultaneously increased the proportion of FOA^R cells to 78%, reflecting a high degree of silencing (Fig. 4). In contrast, targeting of a Rap1p COOH-terminal domain bearing the *rap1-12* mutation, or targeting of full-length Sir4p, Sir3p, or Sir1p, restored strong silencing but failed to reduce the length of the targeted telomere (Fig. 4). Thus, silencing was not sufficient to allow proper length regulation, at least in the context of *rap1-825**. The two strongest silencers, Gbd/rap1-12 and Gbd-Sir4, increased telomere length by an additional 100 bp, exacerbating the length regulation defect of the *rap1-825** allele. Conversely, in the absence of UAS_G sites, the derepression caused by Gbd-Sir1 coincided with telomere shortening (Fig. 4). Silencing and telomere length sensing thus appear to be separate phenomena that use the same COOH-terminal domain of Rap1p but are mutually antagonistic.

Because Rap1p-binding sites occur in native telomeric repeats every 18 bp on average (*13*), our results indicate that the addition of Rap1p molecules on one side of a telomere results in an equivalent loss on the other side of the telomere, which suggests that the number of Rap1p molecules (more specifically, Rap1p COOH-termini) assembled at a telomere is actively maintained at a constant mean value. On the basis of these findings, we propose a simple negative feedback model for telomere length regulation in which a telomere bound by a threshold number of Rap1p molecules (or more) is in a state that prevents telomere elongation, possibly by the assembly of a structure that inhibits telomerase binding or activity. An intermediate target of this signal might be Cdc13p, a single-strand telomeric DNA-binding protein, or Stn1p, a Cdc13p-interacting protein, because both proteins can negatively regulate telomere elongation (*25*). When degradation or incomplete replication of this telomere causes the loss of one or more Rap1p-binding sites, the telomere switches to a new state that allows its elongation. Telomere elongation restores the missing Rap1p-binding site(s), and the telomere switches back to the initial repressed state. This model is in agreement with the extensive telomere elongation observed in cells containing a mutated form of Rap1p lacking its COOH-terminal domain (*9*, *26*).

Additional support for a counting mechanism for telomere length regulation comes from studies of the related yeast *Kluyveromyces lactis* (*8*). Specific mutations in the *K. lactis* telomerase RNA template, which alter telomeric DNA sequences and reduce *K. lactis* Rap1p binding, result in massive telomere elongation after only a few generations. Thus, if telomerase cannot generate Rap1p-binding sites, a threshold number of bound Rap1p is never reached and telomere elongation proceeds unchecked. Our model suggests that telomere elongation is caused by an overall reduction in telomere-bound Rap1p molecules, and not necessarily by the loss of the most distal molecules.

The same domain of Rap1p that regulates telomere length can also establish silencing. However, our results show that the establishment of silencing is neither necessary nor sufficient for length regulation, and may even compete with this second function of Rap1p. Consistent with this idea, the *rap1-12* allele or a deletion of *RIF1* or *RIF2*, two genes encoding Rap1p-interacting factors, increase telomere length but improve telomeric silencing and the Rap1p-Sir4p interaction (*21*, *27*). Conversely, in cells lacking Sir3p or Sir4p, or in which the telomere is transcribed, silencing is lost but telomeres are shortened (*22*, *28*). To explain these observations, we propose that a Rap1p molecule interacting with the Sir proteins, and thus involved in establishing silencing, is not counted as part of the telomere by the length-sensing mechanism. Because a stable Sir3p-Rap1p interaction depends on histone H4 integrity (*20*), telomeric Sir-Rap1 complexes may be restricted to the centromeric side of the telomeric tract where nucleosomes are first encountered (*4*, *5*), leaving the more distal Rap1p molecules free to interact with Rif1p and Rif2p to regulate telomere length. Although changes in the concentration of Sir proteins or their affinity for Rap1p can modify TG_{1-3} length, we propose that the number of Sir-free telomeric Rap1p mole-

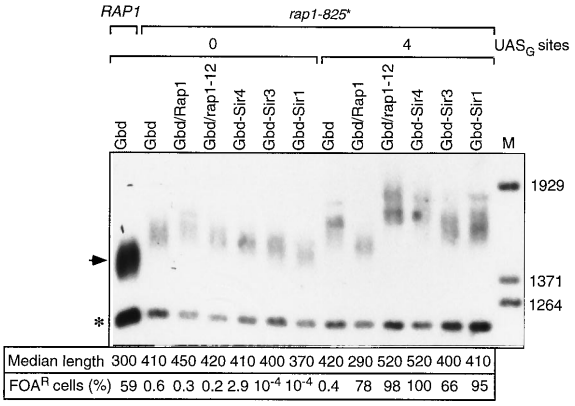

Fig. 4. Gbd/rap1-12, Gbd-Sir4, Gbd-Sir3, and Gbd-Sir1 establish silencing at a telomere but fail to regulate telomere length. Strains Lev7 (no UAS_G sites) and Lev8 (four UAS_G sites) were cotransformed with sp19 (*rap1-825**) and with pSB362 (pGbd), pSB136 (pGbd/Rap1), pSB341 (pGbd/rap1-12), sp138 (Gbd-Sir4), sp131 (Gbd-Sir3), or pKL5 (Gbd-Sir1) and analyzed as above. The median length of the TG_{1-3} tract and the percentage of FOA^R cells are indicated below each lane. Proportions of FOA^R cells were determined as follows: Independent colonies were resuspended in water, diluted to an appropriate concentration, and spread on SC-His and fresh SC-His + 5-FOA plates (5-FOA at 0.8 g/liter). The number of colonies was counted after 4 days at 30°C. Each percentage represents the average of three samples. For means >1%, the SD/mean ratio was <0.17; for means <1%, the ratio was between 0.30 and 1.30. The arrow and asterisk have the same meanings as in Fig. 2.

cules is kept constant.

Because the structural and functional properties of telomeres appear to be highly conserved, our findings may be relevant to telomere length regulation in humans, which has been associated with aging and cancer (*29*). The discovery of human proteins that bind specifically to telomeric repeats (*30*), and more recent functional studies (*31*) on one of these proteins, TRF1, suggest that a protein-counting mechanism similar to that described here may regulate telomere length in human cells.

REFERENCES AND NOTES

1. V. A. Zakian, *Science* **270**, 1601 (1995).
2. J. Lingner, J. P. Cooper, T. R. Cech, *ibid.* **269**, 1533 (1995); J. D. Watson, *Nature New Biol.* **239**, 197 (1972).
3. C. W. Greider and E. H. Blackburn, *Cell* **43**, 405 (1985); *ibid.* **51**, 887 (1987); M. S. Singer and D. E. Gottschling, *Science* **266**, 404 (1994).
4. J. H. Wright, D. E. Gottschling, V. A. Zakian, *Genes Dev.* **6**, 197 (1992); A. J. Lustig, S. Kurtz, D. Shore, *Science* **250**, 549 (1990); F. Klein *et al.*, *J. Cell Biol.* **117**, 935 (1992).
5. M. N. Conrad, J. H. Wright, A. J. Wolf, V. A. Zakian, *Cell* **63**, 739 (1990).
6. C. B. Harley, in *Telomeres,* E. Blackburn and C. Greider, Eds. (Cold Spring Harbor Press, Plainview, NY, 1995), pp. 247–263.
7. R. M. Walmsley and T. D. Petes, *Proc. Natl. Acad. Sci. U.S.A.* **82**, 506 (1985); A. J. Lustig and T. D. Petes, *ibid.* **83**, 1398 (1986).
8. M. J. McEachern and E. H. Blackburn, *Nature* **376**, 403 (1995); A. Krauskopf and E. H. Blackburn, *ibid.* **383**, 354 (1996); S. Buck, thesis, Columbia University (1996).
9. G. Kyrion, K. A. Boakye, A. J. Lustig, *Mol. Cell. Biol.* **12**, 5159 (1992).
10. B. Li and A. J. Lustig, *Genes Dev.* **10**, 1310 (1996).
11. D. E. Gottschling, O. M. Aparicio, B. L. Billington, V. A. Zakian, *Cell* **63**, 751 (1990).
12. Plasmid pADE2 (*11*) was cut with Bam HI and religated, deleting the *ADE2* gene. The resulting plasmid (sp59) was cut with Bam HI, end-filled with Klenow polymerase, and ligated with Eco RI–Xba I end-filled fragment from D1724 (*23*), creating plasmids sp194 (with the two telomeric sequences in opposite orientation) and sp195 (with the two telomeric sequences in the same orientation). Plasmid sp193 (Tel270 in opposite orientation) was created by inserting an Eco RI–Hind III end-filled fragment from pLTel (*13*) into sp59 cut with Bam HI. Yeast strains used in this study are all derivatives of Lev95 (*MAT***a** *ade2-1 trp1-1 leu2-3,112 his3-11,15 URA3-1 can1-100 rap1::LEU2 pRAP1-SUP4-0*), which is itself derived from strain W303-1B. Lev143/144, Lev165/166, and Lev153/154/155 result from the transformation of Lev95 with the linearized plasmids sp194, sp195, and sp193, respectively. Lev7 and Lev8 are described in (*24*).
13. M. S. Longtine, N. M. Wilson, M. E. Petracek, J. Berman, *Curr. Genet.* **16**, 225 (1989); E. Gilson, M. Roberge, R. Giraldo, D. Rhodes, S. M. Gasser, *J. Mol. Biol.* **231**, 293 (1993); E. Gilson *et al.*, *Nucleic Acids Res.* **22**, 5310 (1994).
14. Plasmids pSB362 (Gbd alone), pSB136 (Gbd/Rap1), and pSB341 (Gbd/rap1-12) are based on pRS313 (*HIS3 CENVI*) and contain sequences encoding Gbd fused to the *RAP1* promoter and the 3′ end of *RAP1* from codon 653 (*21*). Plasmids sp138 (Gbd-Sir4) and sp131 (Gbd-Sir3) are described in (*24*), and plasmid pKL5 (Gbd-Sir1) in (*23*). Plasmids sp17 (*RAP1*), sp103 (*rap1-12*), and sp19 (*rap1-825**) are based on pRS313, with the *HIS3* gene disrupted as follows: plasmids LSD135, pSB328 (*21*), and PM585 (*19*) were cut with Nde I, end-filled with Klenow, and religated to give plasmids sp17, sp103, and sp19, respectively. Plasmids sp179 (one UAS_G site) and sp180 (two UAS_G sites) were constructed as follows: UAS_G oligonucleotides (*21*) were end-filled, ligated with a Bgl II linker, cut with Bgl II, and inserted into sp59 cut with Bam HI. A third UAS_G site was ligated with Bgl II–cut sp180 to give plasmid sp181. Lev130, Lev132, and Lev134 result from the transformation of Lev95 with the linearized plasmids sp179, sp180, and sp181, respectively.
15. Overexpression of the COOH-terminal half of Rap1p from a high–copy number plasmid was reported to cause telomere lengthening (*5*) [C. F. J. Hardy, thesis, Columbia University (1991)]. In our experiments, the Gbd/Rap1 hybrid was expressed on a centromere plasmid by means of the *RAP1* promoter, which most likely explains its lack of effect on telomere length in the absence of UAS_G sites.
16. L. Sussel and D. Shore, *Proc. Natl. Acad. Sci. U.S.A.* **88**, 7749 (1991).
17. S. Marcand, E. Gilson, D. Shore, unpublished results.
18. In both wild-type and mutant cells, we observed a nonlinear response with increasing numbers of Gbd/Rap1 hybrids targeted to the telomere. One possible explanation is that full site occupancy may not have been achieved in these experiments, particularly with larger numbers of sites (three or four).
19. P. Moretti, K. Freeman, L. Coodley, D. Shore, *Genes Dev.* **8**, 2257 (1994).
20. G. Kyrion, K. Liu, C. Liu, A. J. Lustig, *ibid.* **7**, 1146 (1993); M. Cockell *et al.*, *J. Cell Biol.* **129**, 909 (1995); A. Hecht, S. Strahl-Bolsinger, M. Grunstein, *Nature* **383**, 92 (1996); C. Liu and A. J. Lustig, *Genetics* **143**, 81 (1996).
21. S. W. Buck and D. Shore, *Genes Dev.* **9**, 370 (1995); C. Boscheron *et al.*, *EMBO J.* **15**, 2184 (1996).
22. F. Palladino *et al.*, *Cell* **75**, 543 (1993).
23. C.-T. Chien, S. Buck, R. Sternglanz, D. Shore, *ibid.*, p. 531.
24. S. Marcand, S. W. Buck, P. Moretti, E. Gilson, D. Shore, *Genes Dev.* **10**, 1297 (1996).
25. C. I. Nugent, T. R. Hughes, N. F. Lue, V. Lundblad, *Science* **274**, 249 (1996); J.-J. Lin and V. A. Zakian, *Proc. Natl. Acad. Sci. U.S.A.* **93**, 13760 (1996); N. Grandin, S. I. Reed, M. Charbonneau, *Genes Dev.*, in press.
26. In *rap1^t* cells, which lack most of the COOH-terminal region of Rap1p, targeting Rap1p COOH-terminal domains to a telomere containing four UAS_G sites is still insufficient to reduce telomere length (*17*); this indicates that a threshold number of Rap1p COOH-terminal domains, not obtained under these conditions, is required to effectively inhibit telomere elongation.
27. C. F. J. Hardy, L. Sussel, D. Shore, *Genes Dev.* **6**, 801 (1992); D. Wotton and D. Shore, *ibid.*, in press.
28. L. L. Sandell, D. E. Gottschling, V. A. Zakian, *Proc. Natl. Acad. Sci. U.S.A.* **91**, 12061 (1994).
29. C. W. Greider, *Annu. Rev. Biochem.* **65**, 337 (1996).
30. L. Chong *et al.*, *Science* **270**, 1663 (1995); T. Bilaud *et al.*, *Nucleic Acids Res.* **24**, 1294 (1996).
31. B. van Steensel and T. de Lange, *Nature*, in press.

32. We thank S. Buck, P. Moretti, D. Gottschling, and R. Rothstein for plasmids and strains; S. Buck for helpful discussions and technical advice; and R. Rothstein, D. Wotton, V. Alvaro, and members of the Gilson lab for comments. Supported by NIH grant GM40094 (to D.S.) and grants from Association pour la Recherche contre le Cancer (ARC), Association Française de Lutte contre la Mucovisidose (AFLM), Ligue Nationale contre le Cancer, and Région Rhônes-Alpes (to E.G.).

1 November 1996; accepted 21 January 1997

Defective Transcription-Coupled Repair of Oxidative Base Damage in Cockayne Syndrome Patients from XP Group G

Priscilla K. Cooper,* Thierry Nouspikel, Stuart G. Clarkson, Steven A. Leadon

In normal human cells, damage due to ultraviolet light is preferentially removed from active genes by nucleotide excision repair (NER) in a transcription-coupled repair (TCR) process that requires the gene products defective in Cockayne syndrome (CS). Oxidative damage, including thymine glycols, is shown to be removed by TCR in cells from normal individuals and from xeroderma pigmentosum (XP)-A, XP-F, and XP-G patients who have NER defects but not from XP-G patients who have severe CS. Thus, TCR of oxidative damage requires an XPG function distinct from its NER endonuclease activity. These results raise the possibility that defective TCR of oxidative damage contributes to the developmental defects associated with CS.

Nucleotide excision repair is an evolutionarily conserved pathway by which cells remove a wide variety of helix-distorting lesions from DNA. It is a complex multiprotein process involving dual incisions on either side of the lesion and removal of an oligonucleotide containing the damage (*1*). Defects in any of seven different human genes (*XPA* through *XPG*) encoding proteins with functions in the early steps of NER result in the hereditary disease xeroderma pigmentosum, characterized by sensitivity to sunlight, marked skin changes in exposed areas, and extreme susceptibility to skin cancer. Cells from patients with another hereditary disease, Cockayne syndrome, are specifically defective in the preferential removal of lesions from transcribed strands of active genes by a TCR process that has

P. K. Cooper, Life Sciences Division, Building 934, Lawrence Berkeley National Laboratory, University of California, 1 Cyclotron Road, Berkeley, CA 94720, USA.
T. Nouspikel and S. G. Clarkson, Department of Genetics and Microbiology, University Medical Center (CMU), 1211 Geneva 4, Switzerland.
S. A. Leadon, Department of Radiation Oncology, University of North Carolina School of Medicine, Chapel Hill, NC 27599–7512, USA.

*To whom correspondence should be addressed.